Alteration and Lithogeochemistry of Altered Rocks at Well KMJ-49 Kamojang Geothermal Field, West Java, Indonesia

D.F.YUDIANTORO[1], EMMY SUPARKA[2], ISAO TAKASHIMA, DAIZO ISHIYAMA[3] AND YUSTIN KAMAH[4]

[1]Geological Engineering UPN "Veteran" Yogyakarta, Indonesia
(Student PhD at Geological Engineering Institute of Technology Bandung, Indonesia)
[2]Geological Engineering Institute of Technology Bandung, Indonesia
[3]Centre for Geo-Environmental Science, Akita University, Japan
[4]Pertamina Geothermal Energy, Indonesia
email: d_fitri4012@yahoo.com

Abstract. Kamojang geothermal field is located in a 1.2 to 0.452 Ma. Quarternary volcanic caldera system. Around the geothermal field, there are several volcanoes (cinder cones) which include: Gunung sanggar, Gunung ciharus, Gunung jawa, Gunung pasir jawa and Gunung cakra (here "gunung" means "mount"). The activity of this volcanic complex contributes greatly to the presence of Kamojang geothermal field, which forming steam dominated system with high temperature around 250°C. The system has capacities of 260 MWe and 140 MWe. Volcanic rocks found around the geothermal field have been altered in general and some of them are difficult to be identified their initial character. Thus, it is necessary to study alteration rocks and lithogeochemistry of a geothermal field. Based on this idea, this study uses some methods consisting of: petrographic, geochemical and alteration box plot analysis. The analyses have been conducted for the surface samples and alteration rocks of cutting from Well KMJ-49. This study is expected to improve the understanding on the characteristics of Kamojang geothermal field.

AI and CCPI calculation results indicate that the surface samples have a value ranging from 20 to 34 AI and CCPI ranges from 63 to73. While subsurface samples have AI values around 15-46 and CCPI ranges from 68 to 86. The relations of CPPI and AI will be reflected in the texture and mineralogy of the type and condition of the rock.

Introduction

Kamojang geothermal field is located in the West java province, which is approximately 60 miles southeast of Bandung. Kamojang geothermal field is bordered by several volcanoes such as Mount gandapura in the east, Mount cakra in north, Mount sanggar, Mount pasir jawa and Ciharus lake in the west and Mount jawa in the south. Geographically, this area is located at 107°47'53"-107°48'8" East Longitude and 7°00'-7°02'10" South latitude. The Kamojang field can be reached through Garut, and from here continue to the north about 21 km. The road condition is quite good until reaching the Kamojang crater where it is also a tourism area (Fig. 1.); Kamojang geothermal field was discovered by the Dutch in 1920 and exploration began in 1973 with cooperation of the Indonesia government and Newzealand. After 10 years exploration, in 1983 field production was 140 MWe, and in 1997 expanded to 220 MWe (Sudarman *et al.*, 1995).

The purpose of this research is to conduct chemical analysis of the alteration rocks and understanding relationship of the alteration minerals. The basic principle of this method is to make a simple chart of the data of lithogeochemistry of alteration rocks. To better understand the relationship between alteration minerals and lithogeochemistry, it can be interpreted in the type of volcanic rock prior to alteration. This method was originally used in the exploration of volcanic-hosted massive sulfide (VHMS) deposits in characterizing the intensity of alteration of volcanic rocks. This method

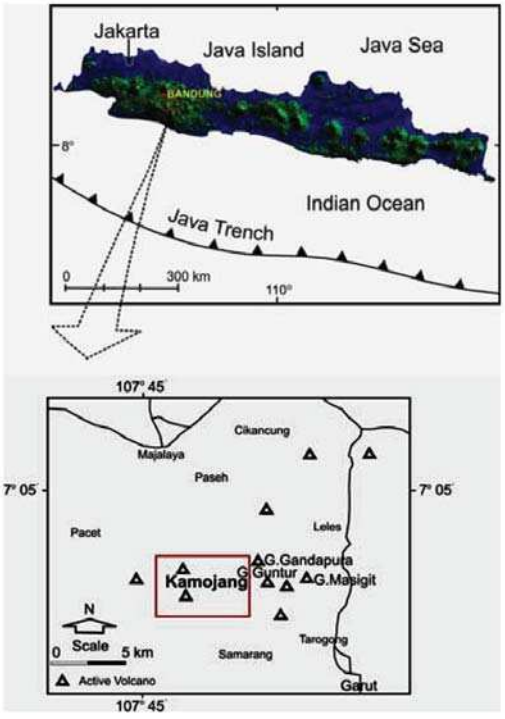

Fig. 1. Location map of research area

was previously proposed by Large *et al*. (2001), Paulick *et al*. (2001) and Herrmann and Hill (2001). In this study, the method was applied to the alteration rock due to hydrothermal processes in the Kamojang geothermal field. The lithogeochemistry analysis was conducted for the surface sample (outcrop) and cutting of alteration rocks of well KMJ-49. Petrographic and X-ray defraction (XRD) analysis was performed to observe the texture and mineralogy composition of the alteration rocks. The rock chemical data was obtained from analysis of X-ray fluorences (XRF), and then analyzed using a method of alteration box plot (Ishikawa *et al*., 1976) to determine the Ishikawa alteration index (AI) and the chlorite-carbonate-pyrite index (CCPI).

According to Ishikawa *et al*. (1976), the alteration box plot is a graphical representation that uses two alteration indices: the Ishikawa alteration index (AI) and the chlorite-carbonate-pyrite index (CCPI).

Ishikawa AI

$$AI = \frac{100(K_2O+MgO)}{(K_2O+MgO+Na_2O+CaO)} \quad \text{.....(1)}$$

This index was defined by Ishikawa *et al*. (1976) to quantify the intensity of sericite and chlorite alteration that occurs in the footwall volcanics proximal to Kuroko deposits. The key reactions measured by the index involve the breakdown of sodic plagioclase and volcanic glass and their replacement by sericite and chlorite. Reactions that describe these alteration processes include:

$3NaAlSi_3O_8 + K^+ + 2H^+ = KAl_3Si_3O_{10}(OH)_2 +$
albite sericite

$6HSiO_2 + 3\ Na^+$ ..... (2)
quartz

and

$2KAl_3Si_3O_{10}(OH)_2 + 3H_4SiO_4 + 9Fe^{2+} + 6Mg^{2+}$
sericite

$+18H_2O = 3Mg_2Fe_3Al_2Si_3O_{10}(OH)_8$ + chlorite

$2K^+ + 28H^+$ ..... (3)

The first reaction is typical of sericite replacement of albite in volcanic rocks in the outer of alteration system (e.g., Date *et al*., 1983; Eastoe *et al*., 1987). The second reaction is important close to massive sulfide mineralization in footwall pipe zones where chlorite-rich assemblage become dominant over sericite-rich assemblage (e.g., Sangster, 1972; Lydon, 1988; Large, 1992; Lentz, 1996; Schardt *et al*., 2001). Reaction (2) involves a loss of Na_2O (and CaO) and a gain of K_2O, whereas reaction (3) involves a loss of K_2O and gains in FeO and MgO, on the basis of constant Al_2O_3. Another equation to complete the above formula is using chlorite-carbonate-pyrite index (CCPI).

$$CCPI = \frac{100\ (MgO + FeO)}{(MgO + FeO + Na_2O + K_2O)} \text{.....} (4)$$

where FeO is total ($FeO + Fe_2O_3$) content of the rock.

Lentz (1996) developed a similar index to study alteration associated with the Brunswick 6 and 12 massive sulfide deposits in the Bathurst mining camp, Canada. The composite ratio used by Lentz ($Fe_2O_{3(total)} + Mg$)/($K_2O + Na_2O$) has been modified in this study (eq 4) to make it comparable to the Ishikawa AI and vary between 0 and 100. One important limitation of this chlorite-carbonate-pyrite index is that it is strongly affected by magmatic fractionation and primary compositional variations in volcanic rocks.

Geology of Kamojang geothermal field. According to Robert (1988), Kamojang geothermal field is located in a large series of volcanoes which lined from the west towards the east including Mount rakutak, Ciharus lake, Pangkalan lake, Mount gandapura, Mount guntur and Mount masigit. Mount rakutak is older than Mount guntur, and both are still active. The development of these volcanoes can be observed through the alignment of magmatic center, and the development of volcanic originated from west to east. Robert, *et al*. (1983) and Robert (1987) indicated that Kamojang field compiled by volcanic deposits which are divided into the Pangkalan and Gandapura units in ascending order. The Pangkalan unit, age 1.20 ± 0.02 Ma, occupies the western part, while the Gandapura unit, age 0.452 ± 0.015 Ma (based on K-Ar method) occupies the eastern Kamojang. According to Kamah *et al.* (2003 and 2005), generally geology of Kamojang geothermal area and surroundings are composed of volcanic deposits of pre and post caldera. The sequence of pre caldera formations are basalt (Mt. Rakutak), basalt (Dog-dog), pyroxene andesite (Mt. Cibereum), pyroclastic (Mt.Sanggar), pyroxene andesite (Mt.Cibatuipis), porphyrytic andesite (Mt.Katomas), basaltic andesite (Legokpulus and Mt.Putri), andesite lava (Mt.Pasir Jawa) and pyroxene andesite (Mt.Kancing) in ascending order. The post caldera formation sequence from old to young are basaltic andesite (Mt.Batususun and Mt.Gandapura), andesite lava (Mt.Gajah), basaltic andesite (Mt.Cakra-Masigit-Guntur). The group of post-caldera formations are unconformity overlying the pre-caldera formations.

Based on outcrop observations in the field, this study divides the lithologic units of the study area into: Basaltic Andesite of Mt. Sanggar, Basaltic Andesite of Mt. Ciharus, Pyroxene Andesite of Mt. Jawa, Pyroclastic Deposits of Mt. Beling, Pyroxene Andesite of Mt. Pasir Jawa and Pyroxene Andesite of Mt. Cakra. The surface and subsurface geology of the area is shown by Fig. 2 and 3. Table-1 describes the relationship between lithology units from several authors.

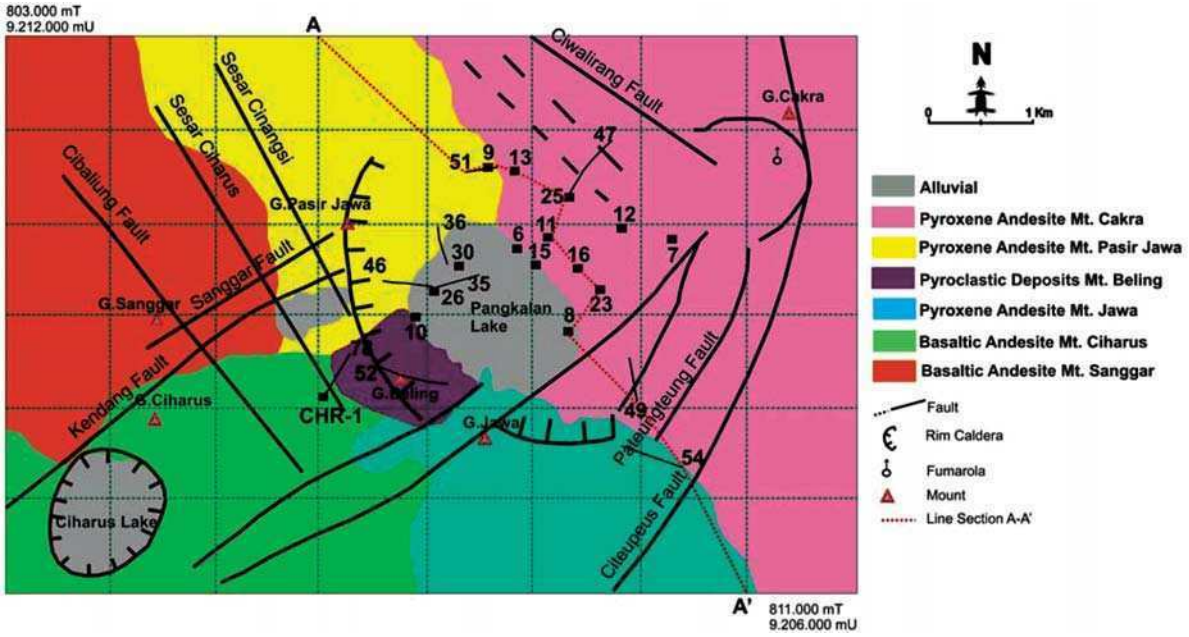

Fig. 2. Geological map of research area (modified from Kamah *et al*., 2003)

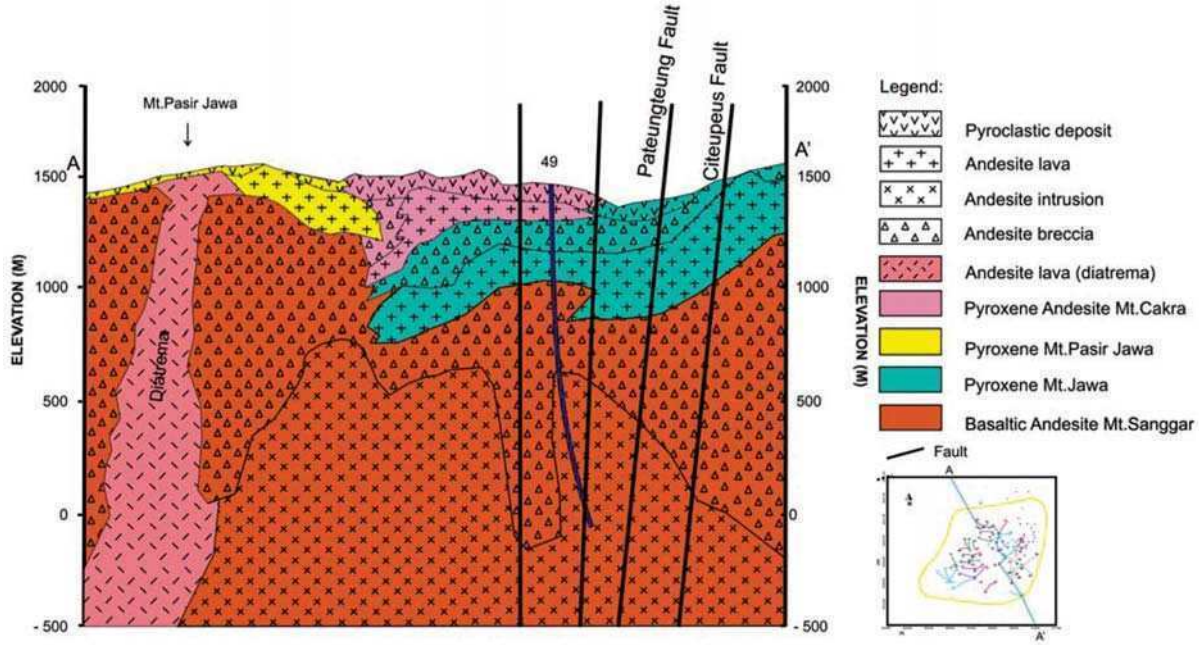

Fig. 3. Cross section A-A' showing the subsurface geology in Kamojang

Table 1. Stratigraphic units of Kamojang area

Robert (1983, 1987)		Kamah *et al.* (2003)		Authors
Lithology Units	Age	Lithology Units		Lithology Units
Gandapura	0.452 Ma	Post Caldera	Basaltic Andesite Mt.Cakra-Masigit & Guntur Andesite Lava Mt.Gajah Basaltic Andesite Mt.Batususun & M.Gandapura	Pyroxene Andesite Mt.Cakra
		Pra Caldera	Pyroxene Andesite Mt.Kancing Andesite Lava Pasir Jawa Basaltic Andesite Mt.Legokpulus & Mt.Putri Pyroxene Andesite Mt.Katomas Pyroxene Andesite Mt.Cibatuipis	Pyroxene Andesite Mt.Pasir Jawa
			Pyroclastic Mt.Sanggar Pyroxene Andesite Mt.Cibereum	Pyroclastic Deposit Mt.Beling Pyroxene Andesite Mt.Jawa Basaltic Andesite Mt.Ciharus Basaltic Andesite Mt.Sanggar
Rakutak	1.2 Ma		Basalt Dog-Dog Basalt Rakutak	

Utami *et al.,* and Browne (1999), Utami (2000) suggests that there are two hydrothermal mineral assemblages present, namely those produced by "acid" and "neutral" pH fluids. The "acid" mineral assemblage which occupies shallow levels (down to 100-300 m) consists of kaoline, smectite, alunite, quartz, cristobalite, and pyrite. The altering fluid was of acid sulphate type formed due to the oxidation of H_2S. The "neutral pH" mineral assemblage occupies deeper levels and comprises varying proportion of quartz, adularia, albite, epidote, titanite, wairakite, laumontite, calcite, siderite, hematite, pyrite, anhydrite, smectite, chlorite, illite, and interlayered clays. The altering fluid was liquid of near neutral pH, and chloride-sulphate type. According to Kamah *et al*. (2003) alteration zone in Kamojang geothermal field can be divided into argillic and propylitic zones. Argillic zone is dominated by clay minerals consisting of kaoline (<120^{o}C), smectite (<150^{o}C) and smectite-illite (>200^{o}C) formed in acidic conditions near neutral (steam zone). The propylitic zone is assemblage of minerals that are in deeper level, has a temperature above 200^{o}C in the reservoir zone. Minerals are present in this zone are epidote, adularia, wairakite, non-swelling chlorite and calcite. Purba (1994) conducted study in well KMJ-48 and KMJ-53 and found the alteration minerals.

Results and Discussion

Texture and mineralogy. The research area is a geothermal field area consists of Quaternary volcanic rocks that altered due to hydrothermal alteration. The alteration rocks were exposed on the surface around the crater with some geothermal manifestations such as: mud pool, steaming ground, fumarola and hot spring. Lava can be found on the walls of the crater and in some places exposed by erosional river water. In this study the samples obtained from surface samples and cutting samples of well KMJ-49 from shallow to the depths. The rock samples were done petrographic and geochemical analysis, whereas XRD analysis conducted on the sample subsurface only. The samples were observed on texture and mineralogical composition. The results of this analysis can be followed as follows:

Surface samples. Petrographic analysis done on 5 samples of volcanic rocks that represent some volcanoes at the research area, which: Mount Sanggar (K-9), Mount Jawa (K-23 and Mount Cakra (K-19, 27 and 35). The petrographic analysis results indicate that there are two types of rocks are: basaltic andesite and andesite pyroxene. Basaltic andesite samples owned by K-9 and the pyroxene andesite samples are K-19, 23, 27 and 35.

Basaltic andesite. Basaltic andesite volcanic rocks exposed at Mount Sanggar (K-9) is lava, gray, fine to medium grained (0.1 to 0.2 cm) with porphyritic texture. The phenocryst composed of plagioclase, pyroxene and opaque minerals are embedded in groundmass volcanic glass. These rocks have experienced partial alterated approximately 8% and alteration minerals are chlorite, clays and iron oxides. Microscopically the basaltic andesite characterized by hypocrystaline, porphyritic, intergranular and intersertal texture. Phenocryst approximately 82-88% sized 0.2 to 1.2 mm and composed by plagioclase, pyroxene and opaque minerals. Groundmass (10-12%) generally composed of fine crystals consisting microlite plagioclase, pyroxene and opaque minerals. Some alteration minerals such as chlorite, clay and iron oxide seems to replace phenocryst on and the edge of the crystal, as well as replace some groundmass. Plagioclase looks colorless, generally present as phenocryst and groundmass approximately 72-75%. The groundmass is fine crystals consisting of Labradorite (An_{53}-An_{58}). Phenocryst sized 0.2 to 0.7 mm with lameral shaped prismatic subhedral-anhedral. Twinning is of Albit and combination Carlsbad-Albit. Some plagioclase shows zoning composition and some individuals of plagioclase phenocryst have been altered and show patches of secondary minerals such as chlorite and clay minerals. Pyroxene (clinopyroxene) is present approximately 5-8% as phenocryst and groundmass, prismatic shape (subhedral-anhderal) with size 0.2 to 0.4 mm. Some pyroxene have been altered, especially on their edge becoming opaque minerals and chlorite and some individual phenocrysts show corrosion by groundmass and inclusions by opaque mineral.

Opaque minerals are present around 5%, as an individual mineral, sometimes in groups and some inclusion pyroxene. In general, opaque minerals present with groundmass. Volcanic glass 10-12% occurs as finely groundmass along with microlite plagioclase and opaque minerals showing intergranular and intersertal texture.

Pyroxene andesite. Pyroxene andesitic lava is found in Mount Jawa (K-23) and Mount Cakra (samples: K-19, 27 and 35). The lava is generally slightly altered approximately 8-12%. In megascopic feature the lava is grey in colour, fine to medium grain size (0.1 to 0.2 cm) with porphyritic texture. Phenocrysts are composed of plagioclase, pyroxene and opaque minerals, embedded in the groundmass of volcanic glass. Chlorite, clay, quartz and iron oxides minerals are present as alteration minerals that alter some plagioclase, pyroxene and groundmass.

Microscopically, part of pyroxene andesite shows scoria structure and generally hypocrystaline porphyritic and intergranular texture. Phenocrysts (82-89%), grain size 0.2 to 1.2 mm, consist of plagioclase, pyroxene and opaque minerals, embedded in the groundmass of volcanic glass (8-15%). Some of plagioclase and pyroxene are inclusion by opaque minerals. Chlorite, clay minerals and opaque (iron oxide) altered some phenocryst on the edge of the crystal and some parts of the groundmass. The amount of alteration minerals is approximately 8-12%. Plagioclase is present approximately 65-72%, colorless, subhedral-anhedral, prismatic, grain size from 0.2 to 1.2 mm, presence as phenocryst and microlite in groundmass. Type of plagioclase is Andesine (An_{45}-An_{49}). Plagioclase phenocrysts generally show twins Albit, Carlsbad-Albit and some individuals show zoning composition. Chlorite and clay minerals are present to

replace some of the edges of plagioclase and crystal fragments. Pyroxene (clinopiroxene) is present about 12-14%, as phenocryst and groundmass, subhedral-anhderal prismatic with size 0.2-0.4 mm. Some pyroxene had been alterated, especially on the edge of crystal becoming opaque minerals and chlorite. Some individual phenocrysts show corrosion by groundmass and opaque mineral inclusion. Opaque minerals present around 3-5%, sometimes grouped in groundmass and partly as pyroxene inclusion. Volcanic glass 8-15% present as finely groundmass with microlite plagioclase and opaque minerals showing intergranular texture.

Subsurface samples. The petrographic and XRD analysis conducted for 17 samples at well KMJ-49 recognizing the presence of some secondary minerals, include:

Crystobalite. Crystobalite is generally present at shallow depths, ie <500 m depth. The presence of crystobalite ranges from 3-25% and the minerals is alteration from some of plagioclase and groundmass.

Quartz. These minerals are present in almost every depth, ranging between 5-55%. This secondary quartz may be present as the result of alteration of plagioclase, pyroxene and groundmass, as well as mineral filler in veins and cavities. As the vein filler, the quartz may be present along with calcite, anhydrite, pyrite and hematite.

Calcite. Calcite is present altering plagioclase, pyroxene and groundmass, and can be present as mineral filler of veins and cavities. Calcite can be occurred with some minerals (Fig. 4a.) such as quartz, epidote, anhydrite and pyrite. The presence of calcite ranging from 5 to 30%.

Anhydrite. Anhydrite is present as the alteration mineral resulted from replacement of plagioclase, pyroxene and groundmass. Besides as alteration mineral, anhydrite fills crystal fracture, cavities or veins along with calcite, gypsum and quartz. Presence less than 12% in the rock and occurring >300 m depth.

Chlorite. Chlorites replace plagioclase, pyroxene and groundmass (Fig. 4b). In plagioclase and pyroxene, chlorite altered the edge or the cleavage crystal. Besides as the mineral alteration, chlorite along with calcite and quartz were present as veins. The presence of chlorite ranges from 5 to 35% in the altered rocks. Chlorite swelling is present at depth less than 900 m, while unswelling chlorite were in >900 m depth.

Epidote. This mineral is present at the depth up to 950 m (Fig. 4b). This mineral is present as replacement of plagioclase and pyroxene. Some of epidote filled veins along with quartz and anhydrite. Epidote is present as alteration mineral around 8%.

Hematite. Hematite occurs as replacement of some of plagioclase, pyroxene and groundmass, and can be present to fill veins and cavities. As vein hematite comes with quartz, pyrite, clays, crystobalite and calcite. Hematite is common in shallow depths and its presence ranges between 3-12%.

Pyrite. This mineral is present in almost any depth. Pyrite occurs replacing mostly pyroxene and groundmass, and can be present as veins mineral along with hematite, quartz and calcite. The content of pyrite ranges between 2-12%.

Clay minerals. These minerals were identified using X-ray diffraction method. In general, these clay minerals are present in the altered rocks and are resulted from alteration of plagioclase, pyroxene and groundmass. Some clay minerals that are present in well KMJ-49 are: montmorillonite, illite-montmorillonite and illite. Montmorillonite is present at shallow depths, i.e <500 m. Some of montmorillonite fills fracture of plagioclase, pyroxene and some veins. Illite-montmorillonite can be found at depths between 500-900 m, along with anhydrite, calcite, quartz, pyrite and hematite. Illite, present at >900 m depths, occurs along with chlorite, epidote, quartz, calcite, hematite and iron oxide.

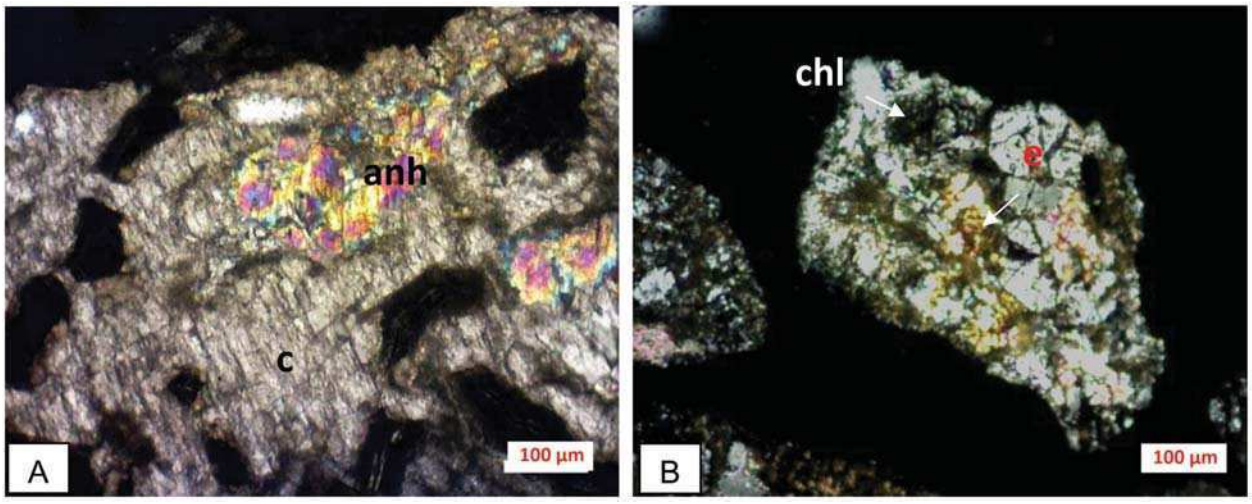

Fig. 4. The figures show some of mineral alterations. A). Calcite (c) and anhydrite (anh) were found at a depth of 674 m. B). Epidote (e) and chlorite (chl) found in the depths of 951 m

Alteration zone. Based on identification of mineral alteration at well KMJ-49, the hydrothermal alteration zones are crystobalite-montmorillonite, illite-montmorillonite and chlorite-epidote zones (Fig. 4-5.). Interpretation of temperature mineral alteration of each zone is shown in Table 2.

Crystobalit-montmorillonite zone. This zone is characterized by the presence of minerals such as crystobalite, montmorillonite, quartz, calcite, anhydrite, gypsum, hematite and pyrite. Minerals are present at <500 m depth formed at temperatures below 100°C (see Table 2).

Table 2. Mineral index temperature of well KMJ-49

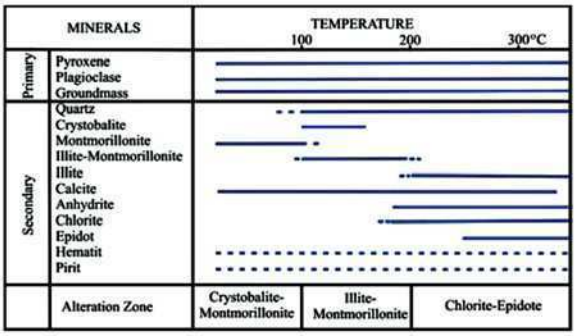

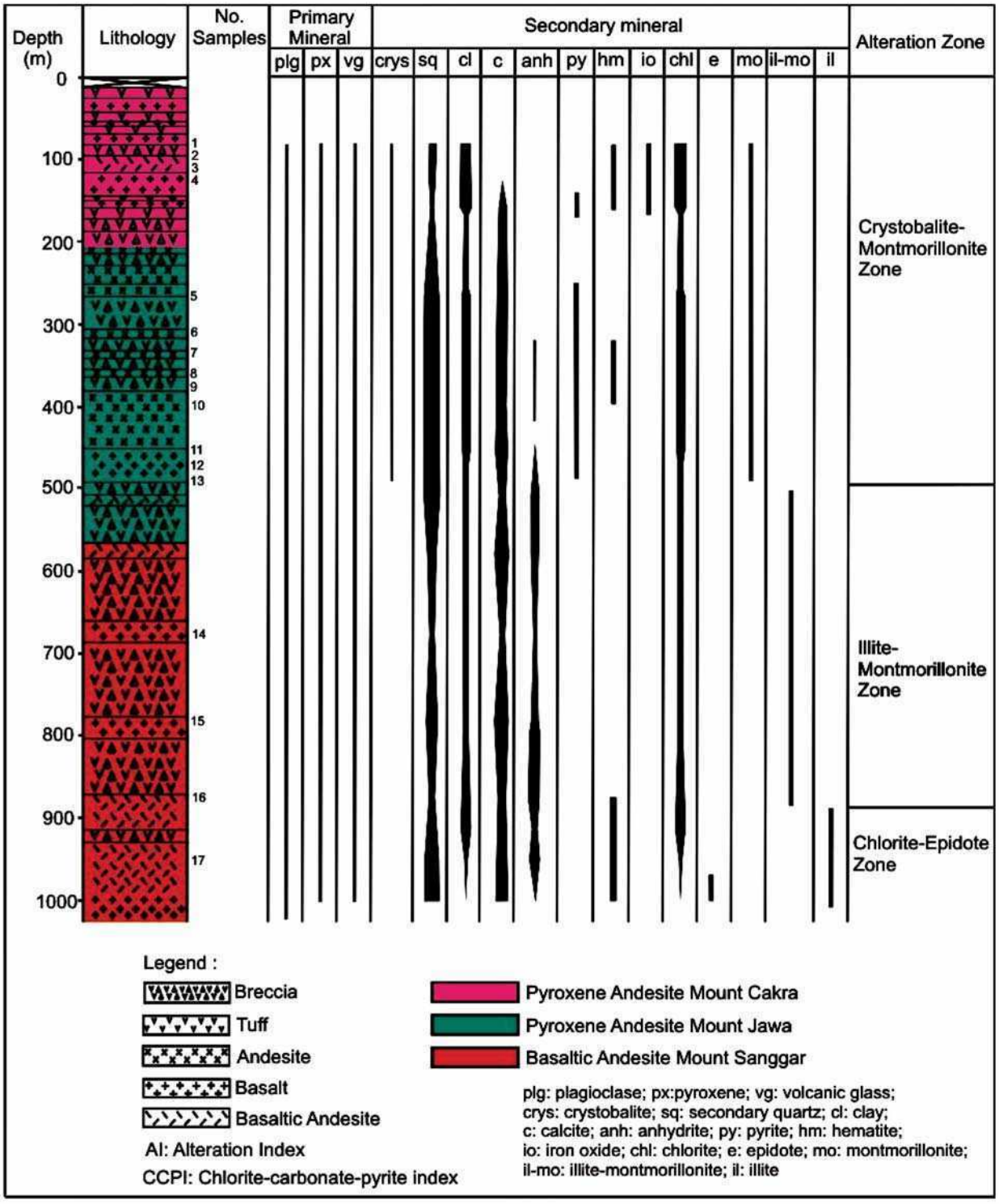

Fig. 5. Composite log of hydrothermal alteration of well KMJ-49

Illite-montmorillonit zone. This zone is characterized by the presence of illite-montmorillonite, calcite, anhydrite, gypsum, hematite and pyrite. Minerals are present at depth ranging from 500-900 m. Temperature interpretation of this zone is based on the formation of crystobalite and montmorillonite minerals ranging between 100-200ºC (see Table 2.).

Chlorite-epidote. This zone is characterized by the appearance of chlorite, epidote, zoisit, illite, wairakit, hematite and pyrite. Minerals are present at > 900 m depth. The temperature of this zone is based on the formation of chlorite and epidote. Minerals are formed at temperatures greater than 200ºC. (see Table 2.). This zone is the reservoir zone with temperature ranging from 235-250ºC (PERTAMINA, 1995).

Alteration box plot. The data needed for this method are the geochemical of altered rocks. Petrographic data required for texture and mineralogy analysis of the altered rocks. Geochemical data should be calculated using equation 1 and 4 to calculate the Ishikawa AI and CCPI. The alteration box plot is a combination of the Ishikawa AI plotted in the horizontal axis and the CCPI plotted in the vertical axis. Least altered volcanic plot toward the center of diagram, and hydrothermal altered volcanic plot at varying positions dependent on the principal hydrothermal mineral present. The mineral end members plot along the boundaries of the box in the position marked.

In this study, geochemical analyzes performed on surface and subsurface rocks in well KMJ-49. The surface samples are needed to compare the surface rock units with subsurface lithology. The analysis has been done so that the distribution of the surface lithology units can be correlated with subsurface lithologies as presented on the geology map (Fig. 2). The location of the surface outcrops and the well KMJ-49 can be seen in Figure 6. The results of calculation of AI and CCPI by applying Formula 1 and 4 were conducted on all samples. The results indicate the surface samples have a value ranging between 20-34 AI and CCPI ranges 63-73. The value of AI is strongly influenced by the mineralogical composition which is composed of plagioclase, pyroxene and volcanic glass as groundmass. Some phenocryst and groundmass appears to be altered into chlorite, clay minerals and iron oxides. The relationship of mineralogy and texture for surface samples seen in the relationship of AI and CPPI is shown in Fig. 6 and 7.

Subsurface samples have AI values around 15-46 and CCPI ranges 68-86. The rock samples have experienced hydrothermal alteration. Plagioclase, pyroxene and volcanic glass occuring as primary minerals have been altered into secondary minerals such as: crystobalite, quartz, calcite, anhydrite, pyrite, hematite, iron oxide, chlorite, epidote, montmorillonite, illite and illite-montmorillonite. The presence of altered minerals is affecting AI and CCPI values of each rock. Corresponding to depths, relative AI values decrease and on the other hand CCPI values increase. This increase is also reflected by the increase in Fe_2O_3 and MgO (see Fig. 8), and are characterized by the presence chlorite, hematite and epidote. AI and CCPI calculation results can be seen in Table 3. The relationship of textures, mineralogy, AI and CPPI is shown Fig. 8.

This study is based on the calculation using Formula 1 and 4, we obtained AI and CCPI values (see Table 3.).

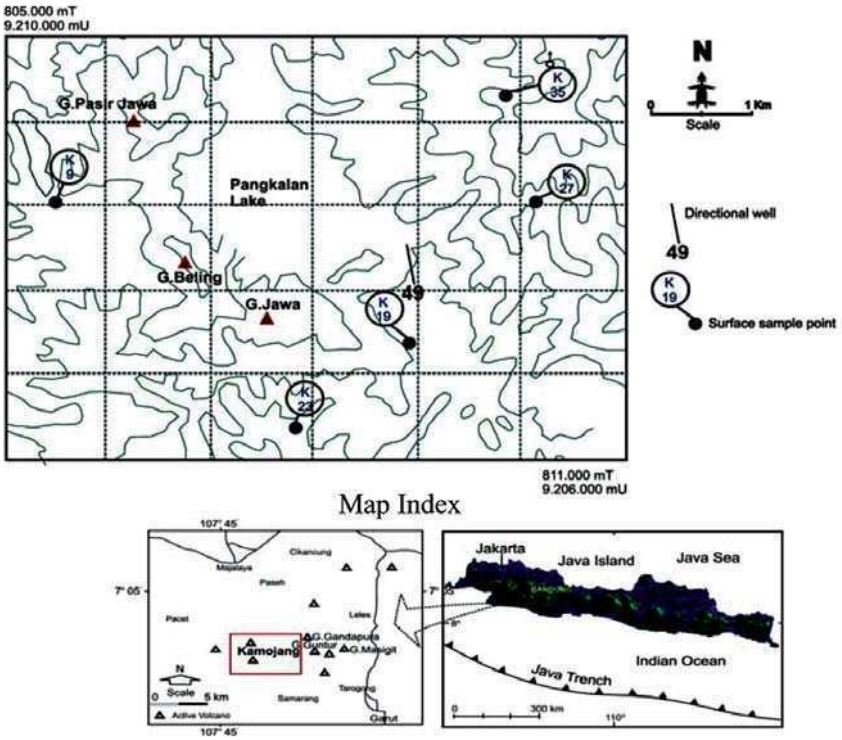

Fig. 6. Locations of the surface samples and well KMJ-49

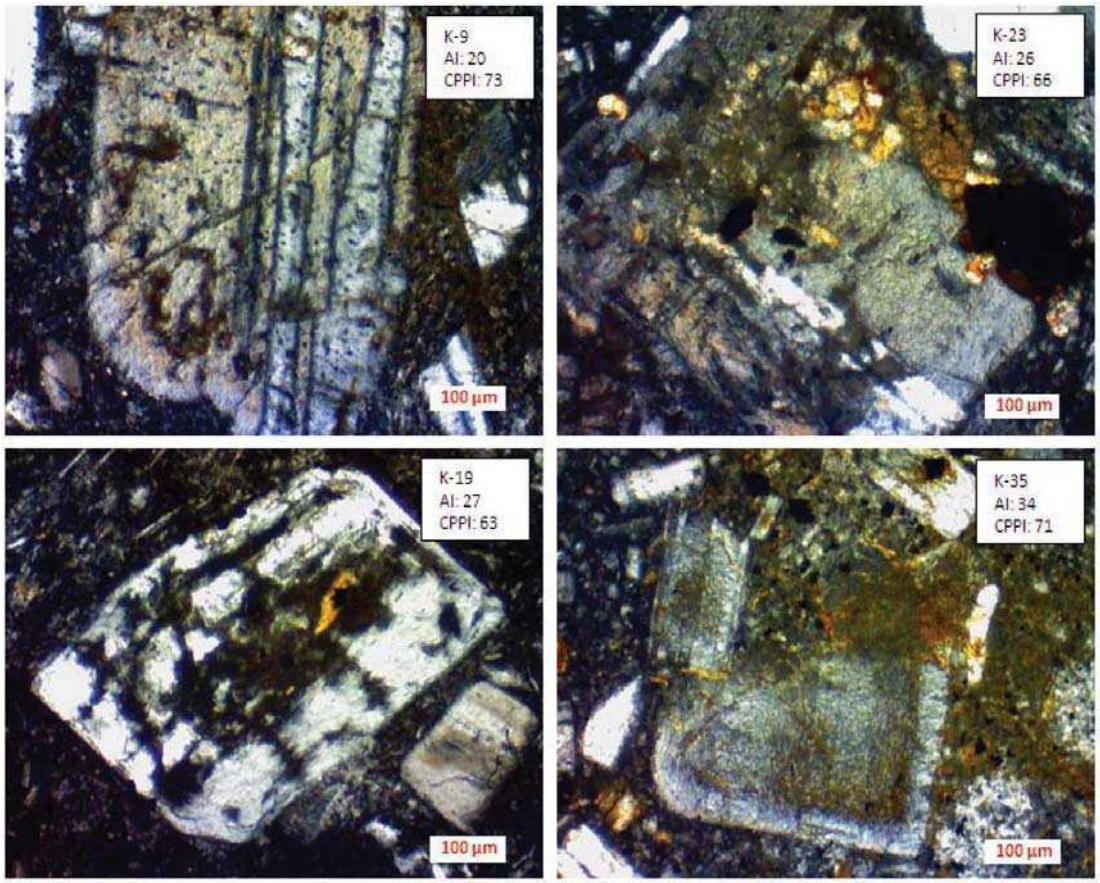

Fig. 7. The relationship of texture, mineralogy, AI and CPPI of the surface samples

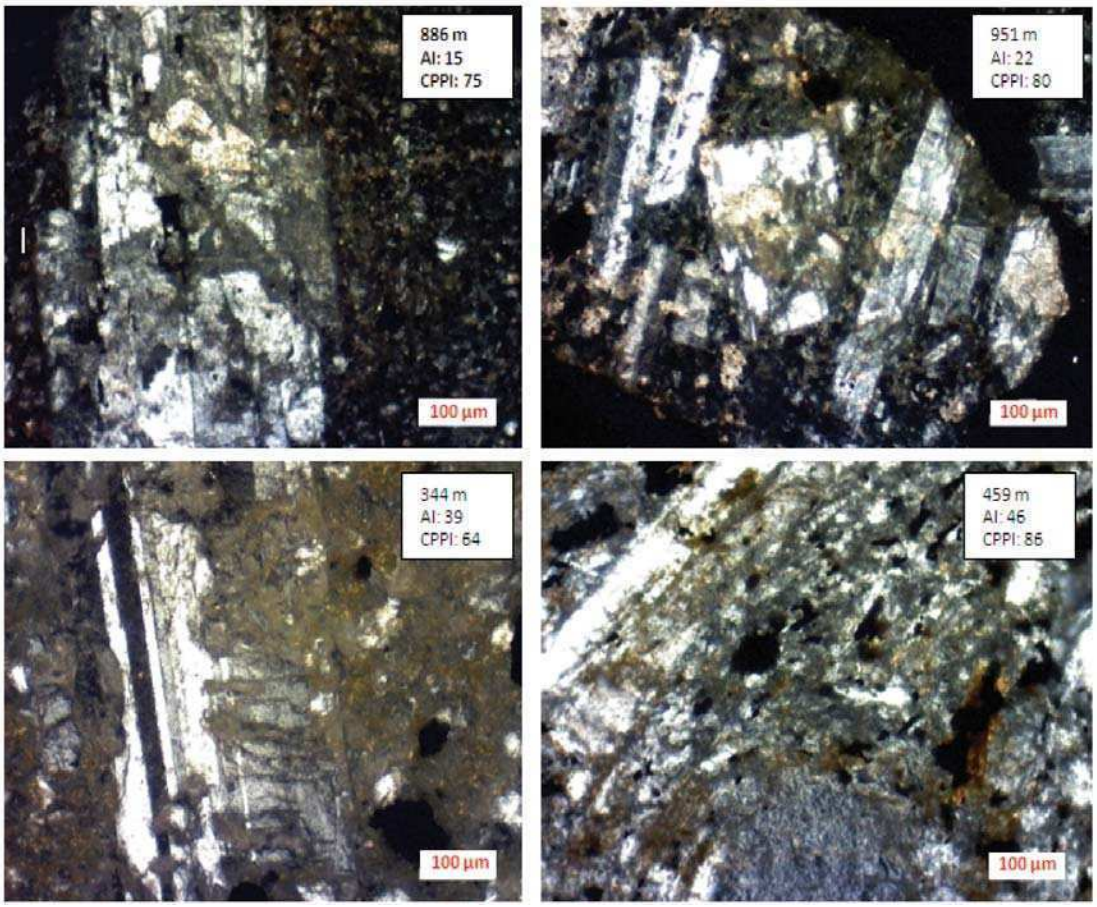

Fig. 8. The relationship of texture, mineralogy, AI and CPPI of the subsurface samples

Table 3. The results of the major elements and Ishikawa alteration index (AI) and chlorite-carbonate-pyrite index (CCPI).

No.	Samples	SiO_2	TiO_2	Al_2O_3	Fe_2O_3	MnO	MgO	CaO	Na_2O	K_2O	P_2O_5	H_2O^-	H_2O^+	IA	CCPI	Rock Name
	Surface															
1	K-9	54.45	0.91	18.50	9.40	0.16	2.12	7.87	3.44	0.77	0.26		1.21	20	73	Basaltic Andesite Mount Sanggar
2	K-27	59.89	0.67	16.18	7.80	0.12	2.38	5.87	2.88	1.61	0.18		2.25	31	69	Pyroxene Andesite Mount Cakra
3	K-35	60.14	0.73	16.06	8.24	0.11	2.57	5.81	2.71	1.73	0.16		1.21	34	71	Pyroxene Andesite Mount Cakra
4	K-23	61.38	0.61	16.63	7.69	0.11	1.54	5.72	3.08	1.55	0.18		1.11	26	67	Pyroxene Andesite Mount Jawa
5	K-19	61.46	0.65	16.91	7.11	0.09	1.24	5.47	2.97	1.87	0.17		1.93	27	63	Pyroxene Andesite Mount Cakra
	Subsurface (well)															
1	Depth (m) 85	51.62	1.06	23.72	4.2	0.04	0.32	2.12	0.66	0.51	0.12	2.92	12.58	23	79	Basalt
2	91	52.61	0.76	26.19	2.18	0.03	0.27	1.05	0.55	0.54	0.06	2.68	13.05	34	69	Basaltic Andesite
3	115	54.3	1.03	21.9	4.56	0.06	1.1	2.49	1.29	1.32	0.17	1.89	9.86	39	68	Basaltic Andesite
4	130	49.3	1.24	18.63	7.04	0.1	1.36	3.2	1.26	1.18	0.18	4.94	11.4	36	77	Basalt
5	296	54.97	0.99	15.61	6.77	0.14	2.56	4.73	1.93	1.63	0.16	2.29	8.2	39	72	Andesite
6	344	59.52	0.78	16.82	6.11	0.11	1.8	3.35	2.48	1.9	0.18	1.93	5	39	64	Andesite
7	350	58.84	0.92	15.13	6.62	0.15	1.92	2.82	1.8	1.97	0.13	3.28	6.38	46	69	Andesite
8	380	56.91	1.24	15	7.01	0.1	1.77	2.64	1.53	1.83	0.21	3.02	8.71	46	72	Andesite
9	386	56.4	1.03	16.23	7.24	0.22	2.67	3.96	2.4	1.42	0.09	1.18	6.96	39	72	Andesite
10	395	56.42	1.06	18.84	7.44	0.18	2.78	6.4	3.04	1.27	0.12	0.77	1.64	30	70	Andesite
11	459	51.44	1.18	17.04	8.59	0.19	2.45	2.15	1.3	0.49	0.14	5.19	10.04	46	86	Basalt
12	471	52.19	1.2	17.28	8.72	0.2	2.48	2.18	1.32	0.49	0.14	5.27	10.19	46	86	Basalt
13	482	47.02	1.22	17.99	9.33	0.21	1.98	4.2	1.66	0.58	1.11	5.84	8.59	30	83	Andesite
14	586	54.31	1.19	16.67	8.07	0.51	1.59	5.24	2.13	0.28	0.15	1.23	7.92	20	80	Basaltic Andesite
15	674	48.47	1.43	16.14	8.89	0.26	3.02	8.47	1.34	0.26	0.17	1.46	10.08	25	88	Basalt
16	787	48.41	1.33	19.97	8.81	0.17	2.85	9	2.49	0.15	0.16	0.33	6.09	21	82	Basalt
17	886	52.11	1.03	21.39	7.18	0.14	1.79	8.38	2.76	0.18	0.27	0.47	4.27	15	75	Basaltic Andesite
18	951	51.8	1.33	17.53	10.21	0.19	2.55	7.28	2.87	0.34	0.15	1.04	4.7	22	80	Basaltic Andesite

AI: Alteration Index
CCPI: Chlorite-carbonate-pyrite index

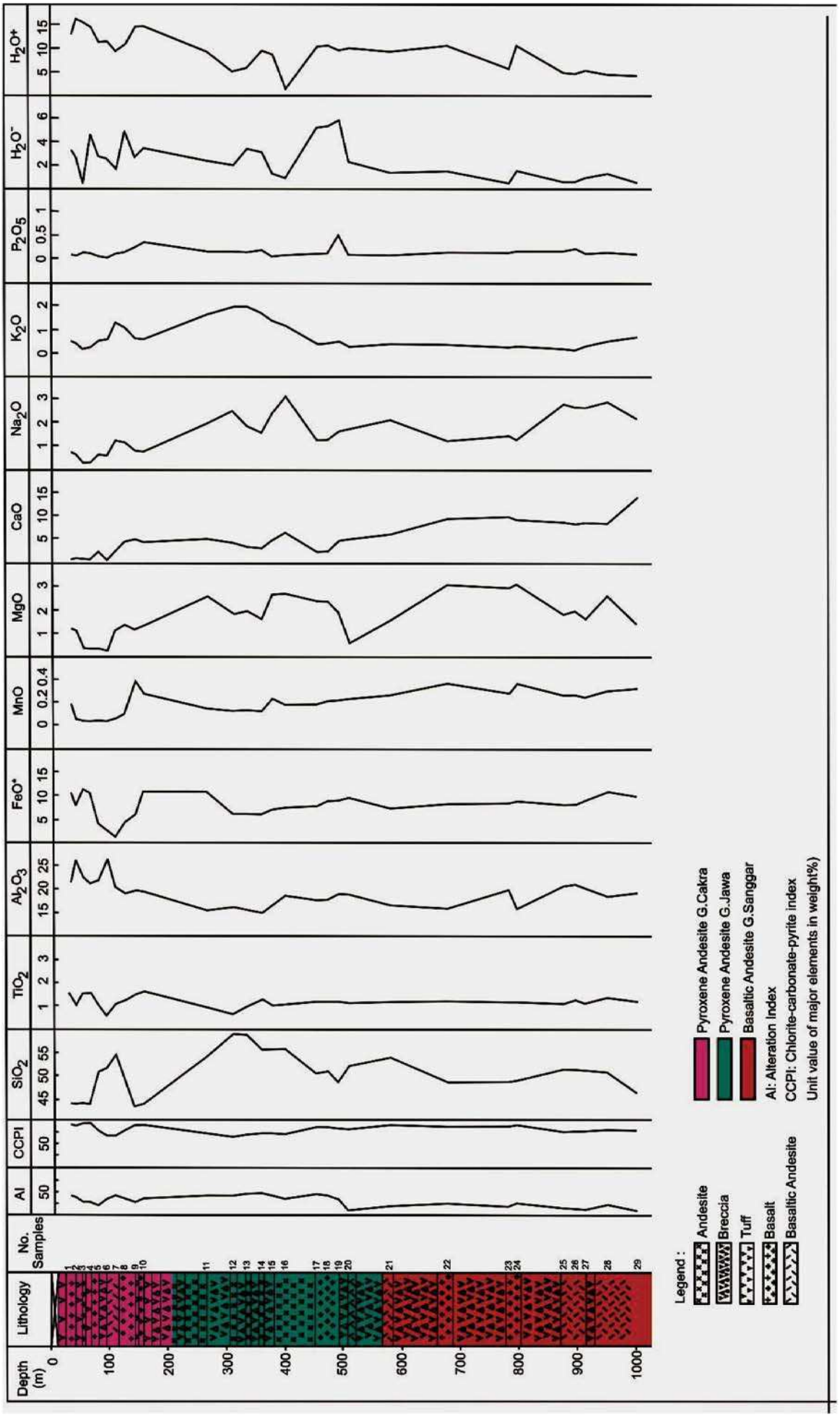

Fig. 9. Log Lithogeochemistry of well KMJ-49

The values then plotted on a simple diagram consisting of the variation between AI and CCPI axis and the variation between the AI with SiO_2. This diagram is intended to determine the origin of rock types prior to alteration. Figure 10 shows the variation between the AI and the CCPI and a box that describes the distribution of rock types. The rock types are andesite/basalt, dacite and rhyolite. At the outer corner of the box is a assemblage of alteration minerals that may be present in the altered rocks. Epidote, calcite are the alteration minerals containing calcium, while chlorite and pyrite are a group of minerals that contains magnesiun and ferrum. Albit and K-feldspar are a group of minerals that contain sodium and potassium.

The resulting plot of the surface and well samples indicate that all the samples were in the box of andesite/basalt types (Fig. 9). While the results of sample plotting on SiO_2 and AI variation diagram show that there are three groups of rocks: basalts (SiO_2 <52%), basaltic andesite (52-55% SiO_2) and andesite (SiO_2> 55%). AI values of each rock groups did not show significant characteristics, each group varies around 15-46 (see Fig. 11). The basaltic andesite is shown in Fig. 11. It shows that the rock types in the group were identical to the lithology units that exposed at the surface as seen in the geological map of the study area. So the distribution of surface rock units is highly correlated with subsurface rock units. It's only at depth of 85-130 m the rock types obtained from plotting AI vs SiO_2 indicate basalt-basaltic andesite, while the exposed rock at the surface around the well KMJ-49 was pyroxene andesite. It is interpreted that the formation of pyroxene andesite of Mount cakra is started by basalt interstratified with basaltic andesite and ended by deposition of pyroxene andesite. The results of plotting the CPPI vs SiO_2 variation diagram explain that all of rock samples processes are caused by the activities of basalt to andesite magmatism composition (Fig. 12).

Conclusion

AI and CCPI calculation conducted on all samples result in as follows: The surface sample had a value ranging

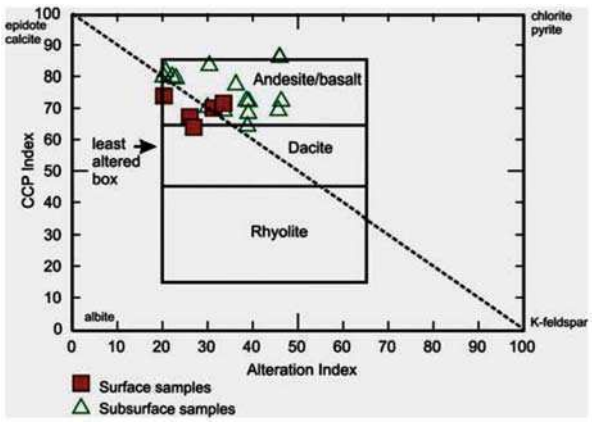

Fig. 10. Variation in Ishikawa AI with CCPI content for a set of least altered volcanic at well KMJ-49.

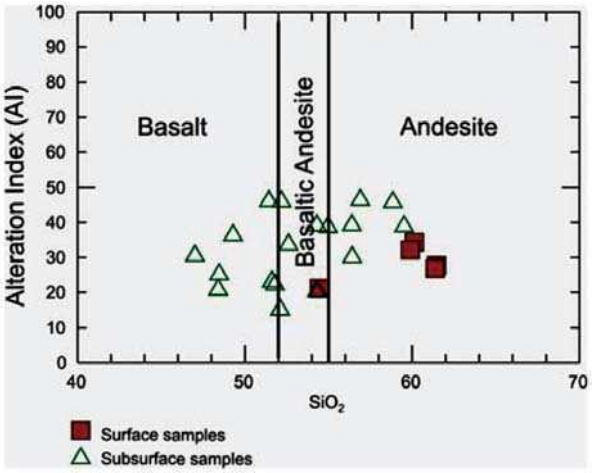

Fig. 11. Variation in Ishikawa AI with SiO_2 content for a set of least altered volcanic at well KMJ-49 (2<Na_2O<5 wt%)

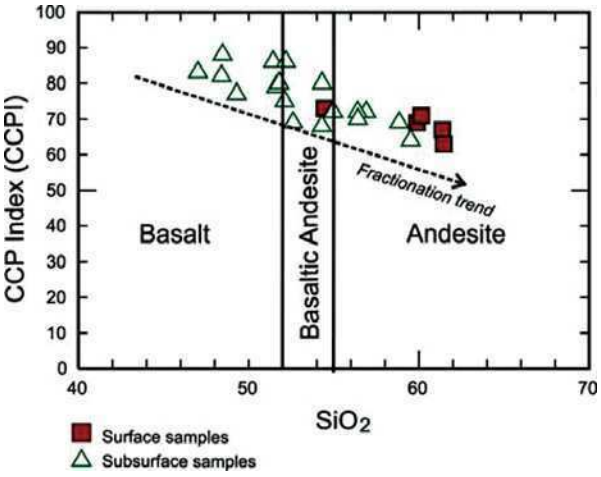

Fig. 12. Variation in CCPI with SiO_2 content

between 20-34 for AI and CCPI range 63-73. Subsurface samples have AI values around 15-46 and CCPI ranges 68-86. All rock samples have experienced hydrothermal alteration. The subsurface samples when observed corresponding to depth indicate the AI values relatively decrease and the CCPI values increase. This increasing is also reflected by the increase of Fe_2O_3 and MgO associated with the presence chlorit, hematite and epidote. The alkali (Na_2O and K_2O) is high (as in samples 5-9) in andesitic rocks, while the lower alkali is occurred in basalt-basaltic andesite. The trending of fractionation from basalt toward andesite is shown by the increasing value of SiO_2 and decreasing of CCPI.

Acknowledgement

The author extends gratitude to Akita University Japan who have given in this research facility and Pertamina Geothermal Energy for permission to publish this paper. I wish to express my appreciation to Dr. C.Prastyadi (Geological Engineering UPN "Veteran" Yogyakarta, Indonesia) for reading the original manuscript and offering many constructive criticisms.

References

Date, J; Watanabe, Y; Saeki, Y. (1983) Zonal alteration around the fukasawa kuroko deposits, akita prefecture, northern Japan: *Economic Geology Monograph*, **5**, p.365-386.

Eastoe, C.J; Solomon, M; Walshe, J.L. (1987) District-scale alteration associated with massive sulfide deposits in the mount read volcanics, western Tasmania. *Economic Geology*, **82**, p.1239-1258

Herrmann, W; Hill, A.P. (2001) The origin of chloride-tremaolite-carbonate rocks associated with the thalanga volcanic-hosted massive sulfide deposit, north Queenland, Australia. *Economic Geology*, **96**, p.1149-1173.

Ishikawa, Y; Sawaguchi, T; Iwaya, S; Horiuchi, M. (1976) Delineation of prospecting targets for kuroko deposits based on models of volcanism of underlying dacite and alteration halos. *Minning Geology*, **26**, p.103-117.

Kamah, Y; Tavip, D; Agus, A.Z. (2003) Penanggulangan problem geologi dalam operasi pemboran sumur di blok timur area geothermal kamojang jawa barat Indonesia. *Proceeding 6Th Indonesian Geothermal Association*, p.175-184.

Kamah, Y.M; Dwikorianto, T; Zuhro, A.A; Sunaryo, D; Hasibuan, A. (2005) The productive feed zones indetified based on spinner data and application in the reservoir potensial review of kamojang geothermal area, Indonesia, *Proceeding World Geothermal Congress Antalya*, Turkey, p.1-6.

Large, R.R. (1992) Australian volcanic-hosted massive sulfide deposits: Features, styles, and genetic models. *Economic Geology*, **87**, p.471-510.

Large, R.R; Allen, R.L; Blake, M.D; Hermann, W. (2001) Hydrothermal alteration and volatile element halos for the rosebery k lens volcanic-hosted massive sulfide deposits, western Tasmania. *Economic Geology*, **96**, p.1055-1072.

Large, R.R; Gemmell, J.B; Paulick, H. (2001) The alteration box plot: A simple approach to understanding the relationship between alteration mineralogy and lithogeochemistry associated with volcanic-hosted massive sulfide deposits. *Economic Geology*, **96**, p.957-971.

Lentz, D.R. (1996) Recent advances in lithogeochemical exploration for massive sulfide deposits in volcanic-sedimentary environments: petrogenetic, chemostratigraphic an alteration aspects with examples from the bathurst camp, new brunswick: new bruswick departement of natural resources and energy. *Mineral and energy division mineral resources report*, 96-1, p.73-119.

Lydon, J.W. (1988) Some observation on the mineralogy and chemical zonation pattern of volcanogenic sulphide deposits of Cyprus. *Geological Survey of Canada Paper*, **84-1A**, p.611-616.

Paulic, H; Herrmamm, W; Gemmel, J.B. (2001) Alteration of felsic volcanics hosting the talanga massive sulfide deposit, north queensland australia, Australia. *Geochemical Proximity Indicators to Ore: Economic Geology*, **96**, p.1175-1200.

PERTAMINA. (1995) Evaluasi kelayakan pengembangan area panasbumi kamojang, laporan internal PERTAMINA divisi panasbumi direktorat eksplorasi dan produksi, *Tim Pokja Kamojang*, 53 pp.

Purba, S. (1994) Hydrothermal alteration of core and cutting samples from wells KMJ-48 and 53 Kamojang. *Geothermal Field West Java Indonesia*, pp. 58.

Robert, D; Raharso, R; Bastaman, S. (1983) Exploration and development of the kamojang. *Geothermal Field, proc. IPA*. p. 171 – 190.

Robert, D. (1987) Geological study of the western part of the kawah kamojang geothermal, *PERTAMINA/BEICIP* report, 89 pp.

Robert, D. (1988) Subsurface study on the optimalisation of the development of the kamojang geothermal field, *BEICIP/ GEOSERVICES, PERTAMINA Divisi Panasbumi (Internal Report)*, 47 pp.

Sangster, D.F. (1972) Precambrium volcanogenic massive sulfide deposits in Canada: A review: *Geological Survey of Canada Paper* 72-22, 44 p.

Schardt, C; Cooke, D.R; Gemmell, J.B; Large, R.R. (2001) Geochemical modeling of the zoned footwall alteration pipe, hellyer volcanic-hosted massive sulfide deposits, westrn Tasmania, Australia. *Economic Geology*, **96**, p.1037-1947.

Sudarman, S. (1983) Geophysical Studies of the Kamojang and Darajat Geothermal Field (Java), *Thesis Master Degree of University of Auckland*, 157 pp.

Sudarman, S; Hochstein, M.P. (1983) Geophysical structure of the Kamojang gothermal field (Java), *Proceeding of 5th NZ Geothermal Workshop*, p. 225 – 230.

Sudarman, S.M; Boedihardi, K; Pastuti, B. (1995) Kamojang geothermal field 10 year operation experience, *Proceeding of WGC*, p.1773-1777.

Utami, P; Browne, P.R.L. (1999) Subsurface hydrothermal alteration in the Kamojang geothermal field west java indonesia, *Proceeding of 24th Workshop on Geothermal Reservoir Engineering*, Stanford University, Stanford California, January 25-27, 1999.

Utami, P. (2000) Characteristics of the Kamojang geothermal reservoir (West Java) as revealed by its hydrothermal alteration mineralogy, *Proceeding of the World Geothermal Congress*, Kyushu-Tohoku, Japan, May 28-June 10, 2000, p.1921-1926.